

Exploring the small mass ratio binary black hole merger via Zeno’s dichotomy approach*

Carlos O. Lousto and James Healy

*Center for Computational Relativity and Gravitation,
School of Mathematical Sciences, Rochester Institute of Technology,
85 Lomb Memorial Drive, Rochester, New York 14623*

(Dated: March 14, 2024)

We perform a sequence of binary black hole simulations with increasingly small mass ratios, reaching to a 128:1 binary that displays 13 orbits before merger. Based on a detailed convergence study of the $q = m_1/m_2 = 1/15$ nonspinning case, we apply additional mesh refinements levels around the smaller hole horizon to reach successively the $q = 1/32$, $q = 1/64$, and $q = 1/128$ cases. Roughly a linear computational resources scaling with $1/q$ is observed on 8-nodes simulations. We compute the remnant properties of the merger: final mass, spin, and recoil velocity, finding precise consistency between horizon and radiation measures. We also compute the gravitational waveforms: its peak frequency, amplitude, and luminosity. We compare those values with predictions of the corresponding phenomenological formulas, reproducing the particle limit within 2%, and we then use the new results to improve their fitting coefficients.

INTRODUCTION

While ground based gravitational wave detectors like LIGO [1] are particularly sensitive to comparable (stellar) mass binaries, third generation (3G) ground detectors [2] and space detectors, like LISA, will also be sensitive to the observation of very unequal mass binary black holes [3]. These will allow the search and study of intermediate mass black holes, either as the large hole in a merger with a stellar mass black hole (a source for 3G detectors) or as the smaller hole in a merger with a supermassive black hole (a source for LISA). The evolution of these small mass ratio binaries has been approached via perturbation theory and the computation of the gravitational self-force exerted by the field of the small black hole on itself [4]. The resolution of the binary black hole problem in its full nonlinearity have been only possible after the 2005 breakthroughs in numerical relativity [5–7], and a first proof of principle have been performed in [8] for the 100:1 mass ratio case, following studies of the 10:1 and 15:1 [9] ones. In the case of [8] the evolution covered two orbits before merger, and while this proved that evolutions are possible, practical application of these gravitational waveforms requires longer evolutions. Other approaches to the small mass ratio regime have recently been followed [10, 11]. Here we report on a new set of evolutions that are based on the numerical techniques refined for the longterm evolution of a spinning precessing binary with mass ratio $q = m_1/m_2 = 1/15$ [12]. We study here the case of a nonspinning $q = 1/15$ binary in a convergence sequence to assess numerical and systematical errors. We then add a sequence of $q = 1/32$, $q = 1/64$, and $q = 1/128$, nonspinning binaries evolutions for about a dozen orbits before merger.

SIMULATIONS’ RESULTS

For the $q = 1/15$ case, we performed three globally increasing resolution simulations labeled by its number of points per total mass $m = m_1 + m_2$, n084, n100, n120, at the waveform extraction zone, about $100 - 150m$ away from the binary. All extracted waveforms are then extrapolated to infinity (\mathcal{S}^+) using Ref. [13] formulas. The medium resolution “n100” simulation has 40 grid points across a radius of $0.08m$ for a finest resolution of $m/512$ at the innermost refinement level around the smaller hole. The whole grid consists of 12 refinement levels with an outer boundary at $400m$ and in the wavezone, the resolution is $m/1.0$. The n084 (n120) simulation has globally decreased (increased) resolution of $m/430.1$ ($m/614.4$) at the finest level. The simulations start at a coordinate separation $D = 8.5m$, or about a simple proper horizon distance (along the coordinate line joining the holes), $SPD=10.1m$. The inspiral evolution follows for about 10 orbits (about $t = 1350m$) before merger and forms a final black hole with the characteristics summarized in Table I. The n100 simulation proceeded at a speed of $2.2m/hr$ on 8 of TACC’s (<https://www.tacc.utexas.edu>) stampede2 nodes, costing approximately 5,340 node hours. To compute black holes masses and spins we use the isolated horizons technique [14], that produces very accurate results compared to radiative computations [15].

Table I displays the convergence rates for all the radiative quantities derived from the gravitational waveform. The detail of the convergence of the waveform phase and amplitude with global numerical resolution is shown in Fig. 1 displaying an 8th order convergence rate (alignment not enforced).

The high convergence of these results allow us to use the medium of the resolutions, n100, as the reference grid to perform a set of smaller q simulations, each time halving the mass ratio and adding a new refine-

TABLE I. The energy radiated, E_{rad}/m , angular momentum radiated J_{rad}/m^2 , recoil velocity v_m , and the peak luminosity $\mathcal{L}_{\text{peak}}$, waveform frequency $\omega_{22}^{\text{peak}}$ at the maximum amplitude h_{peak} , for each resolution of the $q = 1/15$ simulations, starting at $\text{SPD}=10m$. All quantities are calculated from the gravitational waveforms. Extrapolation to infinite resolution and order of convergence is derived.

resolution	E_{rad}/m	J_{rad}/m^2	v_m [km/s]	$\mathcal{L}_{\text{peak}}$ [ergs/s]	$m\omega_{22}^{\text{peak}}$	$(r/m)h_{\text{peak}}$
n084	0.002366	-0.029385	31.45	1.585e+55	0.2906	0.08471
n100	0.002418	-0.029945	33.54	1.649e+55	0.2863	0.08485
n120	0.002436	-0.030097	34.24	1.665e+55	0.2882	0.08489
$n \rightarrow \infty$	0.002444	-0.030148	34.56	1.670e+55	0.2897	0.08489
order	6.19	7.58	6.41	8.11	4.71	8.83

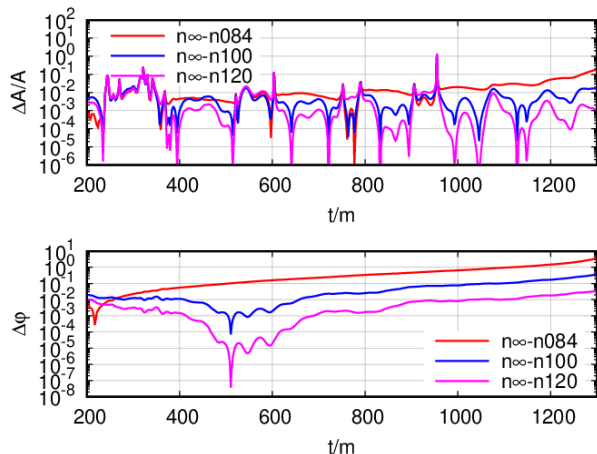


FIG. 1. Difference between each resolution of the $q = 1/15$ strain waveform with the calculated infinite resolution waveform for the amplitude and phase of the (2,2) mode.

ment level around the smaller hole (12, 13, 14, 15 levels for $q = 1/15, 1/32, 1/64, 1/128$, respectively). This basic grid configuration ensures exactly the same accuracy around the larger hole, the radiation and boundary zones, and in between the holes, while doubling the resolution around the smaller hole in such a way that the number of points per horizon remains the same and guarantees its accuracy. We monitor this assumption by verifying the conservation of the small horizon mass (and spin) to within the required accuracy of about one part in 10^4 . In order to maintain the accuracy at this base resolution and account for the longer merger time scale we reduce the initial distance (and hence the evolution time) as shown in Table II. This table displays the final black hole remnant and peak waveform properties, and the consistency between the horizon measures of the final mass and spin with the energy and angular momentum carried out by the gravitational waveforms.

Figure 2 makes a comparative display of the four q waveforms, (2,2)-modes of the strain, in the same scale to show the differences in merger amplitude and evolution time. While Fig. 3 displays the comparative merger time

from a fiducial initial orbital frequency $m\Omega_i = 0.0465$ (corresponding roughly to coordinate separation $D = 7m$ and simple proper distance $\text{SPD} = 8.5m$) to merger for the mass ratios $q = 1/15, 1/32, 1/64, 1/128$ simulations. We observe a time to merger $t_m \sim (83.2 \pm 8.5)m\eta^{-0.56 \pm 0.03}$ dependence for small mass ratios, and interpret it as a composed power of the leading rates from the post-Newtonian regime [16]: q^{-1} from the inspiral decay and q^0 from the plunge.

The simulations of $q = 1/32, 1/64, 1/128$ use an 8th order stencil in space [17] and 4th order in time (with $dt = dx/4$) and have all been performed in TACC's Frontera cluster on 8 nodes (448 cores) at speeds of 1.1, 0.6, and 0.32 m per hour totaling 13,807, 17,713, and 41,250 node hours respectively. Thus showing a notable approximately linear scaling with the mass ratio.

COMPARISONS WITH PREDICTIONS

An important test of accuracy of our simulations is to compare the final properties in Table II versus the predictions of the formulas obtained in Ref. [18] for them. We display these results in Fig. 4. We stress that in this figure there is no fitting being performed to the new data, but a raw comparison of the previous formulas extrapolated to a previously uncovered region of small q .

In the light of these good results, we can now use the current data to generate a new fit of the nonspinning binary remnant and merger waveform properties. We will also correct for the center of mass motion [19, 20] in these new fits, of particular relevance for comparable masses, which was not included for all quantities in Ref. [18]. In practice, the center of mass motion for these nonspinning systems is small, and primarily only affects the recoil velocity. We find that after correction, the recoil velocities change by at most 2%, well within the error from finite resolution (5-10%).

For the unequal mass expansion of the final mass and spin of the merged black holes we will use the forms from [21] that include the particle limit. The fitting formula

TABLE II. Final properties for the sequence of the $q = 1/15, 1/32, 1/64, 1/128$ simulations includes the final black hole mass M_{rem}/m and spin α_{rem} , the recoil velocity v_m , and the peak luminosity $\mathcal{L}_{\text{peak}}$ and waveform frequency $\omega_{22}^{\text{peak}}$ at the maximum amplitude h_{peak} . Also given are the initial simple proper distance, SPD, number of orbits to merger N , and a consistency check of the differences between the final mass and spin, $\Delta M_{\text{rem}}/m$, $\Delta\alpha_{\text{rem}}$, calculated from the horizon and from the radiated energy and angular momentum.

q	M_{rem}/m	$\Delta M_{\text{rem}}/m$	α_{rem}	$\Delta\alpha_{\text{rem}}$	v_m [km/s]	$\mathcal{L}_{\text{peak}}$ [ergs/s]	$m\omega_{22}^{\text{peak}}$	$(r/m)h_{\text{peak}}$	SPD/ m	N
1/15	0.9949	9×10^{-5}	0.1891	2.3×10^{-4}	34.24	1.665e+55	0.2882	0.0849	10.13	10.01
1/32	0.9979	3×10^{-5}	0.1006	2.5×10^{-3}	9.14	4.260e+54	0.2820	0.0424	9.51	13.02
1/64	0.9990	5×10^{-7}	0.0520	2.8×10^{-4}	2.34	1.113e+54	0.2812	0.0220	8.22	9.98
1/128	0.9996	4×10^{-5}	0.0239	2.7×10^{-3}	0.96	3.313e+53	0.2746	0.0116	8.19	12.90

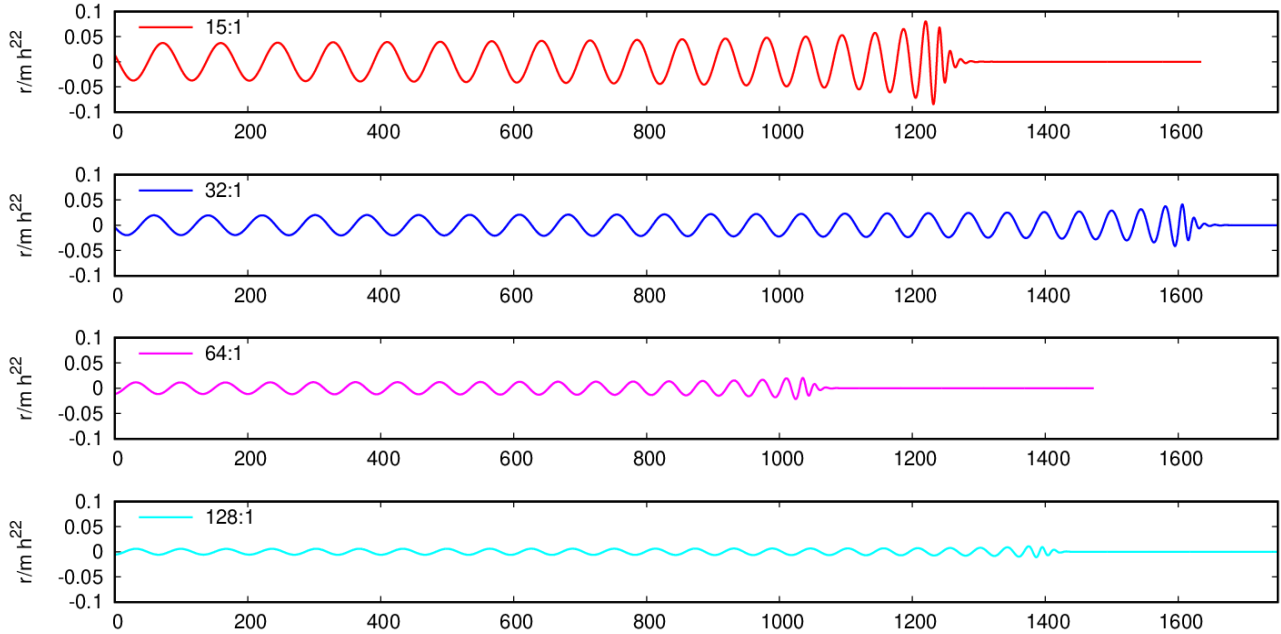


FIG. 2. (2,2) modes (real part) of the strain waveforms versus time (t/m), for the $q = 1/15, 1/32, 1/64, 1/128$ simulations.

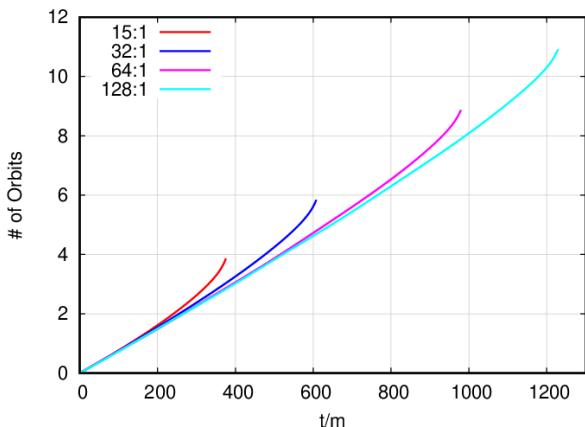


FIG. 3. Comparative number of orbits and time to merger, from a fiducial orbital frequency $m\Omega_i = 0.0465$ for the $q = 1/15, 1/32, 1/64, 1/128$ simulations.

for M_{rem} is given by,

$$\frac{M_{\text{rem}}}{m} = (4\eta)^2 \left\{ M_0 + K_{2d} \delta m^2 + K_{4f} \delta m^4 \right\} + \left[1 + \eta(\tilde{E}_{\text{ISCO}} + 11) \right] \delta m^6, \quad (1)$$

where $\delta m = (m_1 - m_2)/m$ and $m = (m_1 + m_2)$ and $4\eta = 1 - \delta m^2$.

And the fitting formula for the final spin has the form,

$$\alpha_{\text{rem}} = \frac{S_{\text{rem}}}{M_{\text{rem}}^2} = (4\eta)^2 \left\{ L_0 + L_{2d} \delta m^2 + L_{4f} \delta m^4 \right\} + \eta \tilde{J}_{\text{ISCO}} \delta m^6. \quad (2)$$

Note that the two formulae above impose the particle limit by including the ISCO dependencies, $\tilde{E}_{\text{ISCO}}(\alpha_{\text{rem}})$, and $\tilde{J}_{\text{ISCO}}(\alpha_{\text{rem}})$ (See Ref. [21, 22] for the explicit expressions).

For the nonspinning recoil we will use Ref. [18]

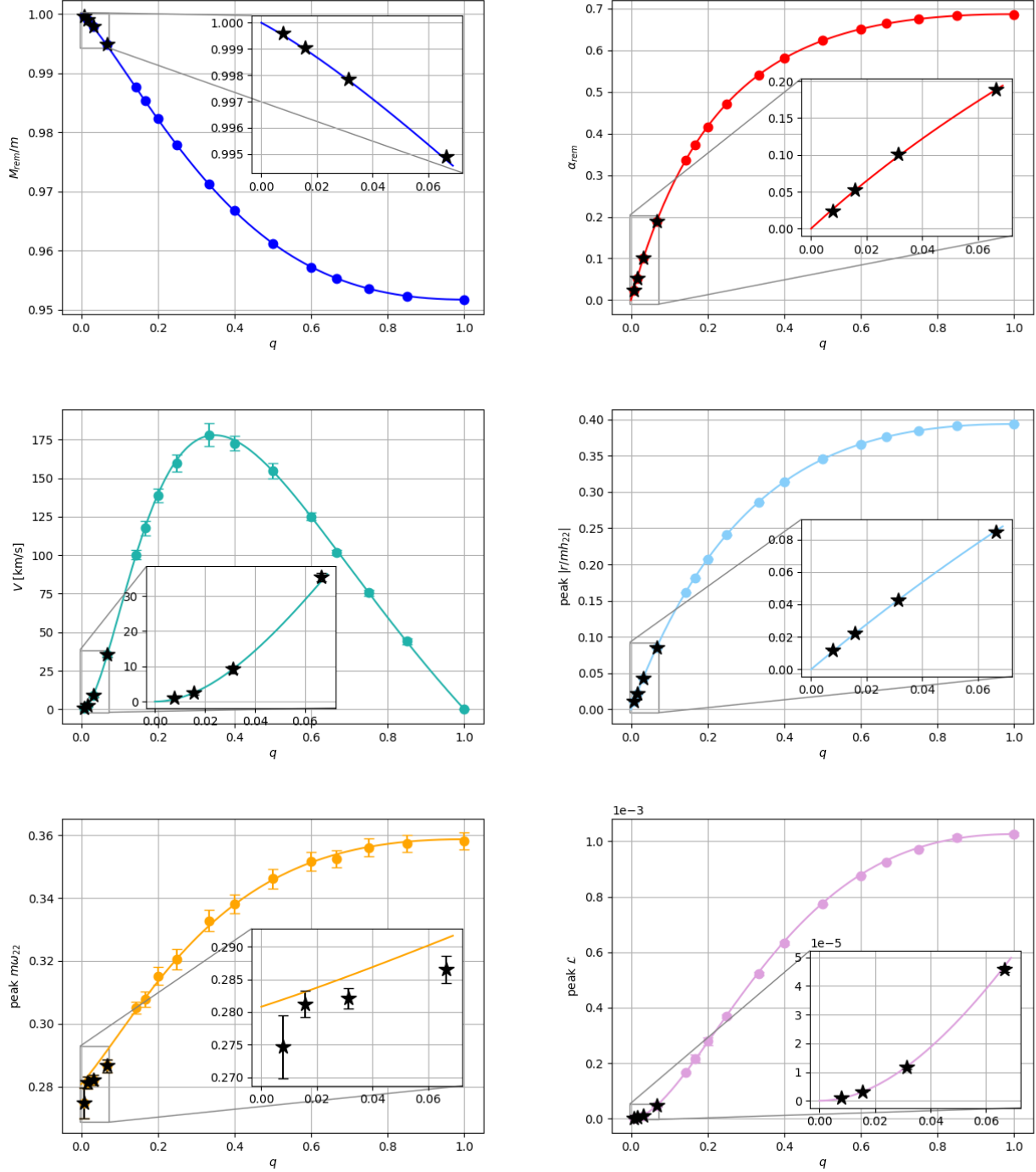


FIG. 4. Final mass, spin, recoil velocity, peak amplitude, frequency, and luminosity. Predicted vs. current results for the $q = 1/15, 1/32, 1/64, 1/128$ simulations. Each panel contains the prediction from the original fits in Ref. [18] (solid line), data used to determine the original fits (filled circles), and the data for the current results (stars). An inset in each panel zooms in on the new simulations. Again, we stress no fitting to the new data is performed in this plot.

parametrization,

$$v_m = \eta^2 \delta m (A + B \delta m^2 + C \delta m^4). \quad (3)$$

We model the peak amplitude (of the strain h) from

the merger of nonspinning binaries using the expansion [23],

$$\left(\frac{r}{m}\right) h_{\text{peak}} = (4\eta)^2 \left\{ H_0 + H_{2d} \delta m^2 + H_{4f} \delta m^4 \right\}$$

TABLE III. Fitting coefficients of the phenomenological formulas (1)-(6)

M_0	K_{2d}	K_{4f}
0.95165 ± 0.00002	1.99604 ± 0.00029	2.97993 ± 0.00066
L_0	L_{2d}	L_{4f}
0.68692 ± 0.00065	0.79638 ± 0.01086	0.96823 ± 0.02473
A	B	C
-8803.17 ± 104.60	-5045.58 ± 816.10	1752.17 ± 1329.00
$N_0 \times 10^3$	$N_{2d} \times 10^4$	$N_{4f} \times 10^4$
(1.0213 ± 0.0004)	(-4.1368 ± 0.0652)	(2.46408 ± 0.1485)
W_0	W_{2d}	W_{4f}
0.35737 ± 0.00097	0.26529 ± 0.01096	0.22752 ± 0.01914
H_0	H_{2d}	H_{4f}
0.39357 ± 0.00015	0.34439 ± 0.00256	0.33782 ± 0.00584

$$+ \eta \tilde{H}_p \delta m^6, \quad (4)$$

where $\tilde{H}_p(\alpha_{\text{rem}})$ is the particle limit, taking the value $H_p(0) = 1.4552857$ in the nonspinning limit [24].

The formula to model the peak luminosity introduced in [23] takes the following simple form for nonspinning binaries,

$$\mathcal{L}_{\text{peak}} = (4\eta)^2 \left\{ N_0 + N_{2d} \delta m^2 + N_{4f} \delta m^4 \right\}. \quad (5)$$

Analogously, we model the peak frequency of the (2, 2) mode of the gravitational wave strain for nonspinning binaries as,

$$m\omega_{22}^{\text{peak}} = (4\eta) \left\{ W_0 + W_{2d} \delta m^2 + W_{4f} \delta m^4 \right\} + \tilde{\Omega}_p \delta m^6, \quad (6)$$

where $\tilde{\Omega}_p(\alpha_{\text{rem}})$ is the particle limit, taking the value $\tilde{\Omega}_p(0) = 0.279525$ in the nonspinning limit [24].

Table III summarizes the new values of all those coefficients with their estimated errors.

CONCLUSIONS

This study represents a new Numerical Relativity milestone for comparative studies to assess improvements in code efficiency, on gauge choices, and on improved initial data, and it allows us to begin considering massive production of small mass ratio simulations to populate the next release of the RIT public catalog of binary black hole waveforms (<https://ccrg.rit.edu/~RITCatalog>). In particular, the simulation of mass ratio 128:1 presented here is a record breaking Numerical Relativity run and it includes nearly 13 orbits before merger. The particle limit remnant and peak waveform parameters are reproduced here within 1%-2% errors using purely full numerical methods and consistency of horizon and radiation

computations has been verified to high precision. The extension to include (high) spins into the large black hole seems straightforward with our current techniques [25] as well as to longer integrations times (with a fourth order Runge-Kutta method), where errors can be controlled by the reduction of the Courant factor. Those sort of improved simulations could be used for direct parameter estimation of direct observations by advanced, 3rd generation ground based gravitational wave detectors and by the space project LISA.

The authors thank N.Rosato and Y.Zlochower for discussions, and also gratefully acknowledge the National Science Foundation (NSF) for financial support from Grant No. PHY-1912632. Local computational resources were provided by the NewHorizons, BlueSky Clusters, and Green Prairies at the Rochester Institute of Technology, which were supported by NSF grants No. PHY-0722703, No. DMS-0820923, No. AST-1028087, No. PHY-1229173, and No. PHY-1726215. This work used the Extreme Science and Engineering Discovery Environment (XSEDE) [allocation TG-PHY060027N], which is supported by NSF grant No. ACI-1548562; and the Frontera projects PHY-20010 and PHY-20007, an NSF-funded petascale computing system at the Texas Advanced Computing Center (TACC).

* The title refers to our approach of halving and halving the mass ratio while adding internal grid refinement levels to the well studied $q = 1/15$ case, inspired by the first of Zeno's paradoxes, as reported by Aristotle [26].

J.L.Borges [27], in *Death and the Compass*, writes "I know of a Greek labyrinth which is a single straight line. Along this line so many philosophers have lost themselves..."

- [1] B. P. Abbott *et al.* (LIGO Scientific, Virgo), Phys. Rev. **D100**, 104036 (2019), arXiv:1903.04467 [gr-qc].
- [2] M. Pürrer and C.-J. Haster, Phys. Rev. Res. **2**, 023151 (2020), arXiv:1912.10055 [gr-qc].
- [3] J. R. Gair, S. Babak, A. Sesana, P. Amaro-Seoane, E. Barausse, C. P. Berry, E. Berti, and C. Sopuerta, J. Phys. Conf. Ser. **840**, 012021 (2017), arXiv:1704.00009 [astro-ph.GA].
- [4] L. Barack and A. Pound, Rept. Prog. Phys. **82**, 016904 (2019), arXiv:1805.10385 [gr-qc].
- [5] F. Pretorius, Phys. Rev. Lett. **95**, 121101 (2005), gr-qc/0507014.
- [6] M. Campanelli, C. O. Lousto, P. Marronetti, and Y. Zlochower, Phys. Rev. Lett. **96**, 111101 (2006), gr-qc/0511048.
- [7] J. G. Baker, J. Centrella, D.-I. Choi, M. Koppitz, and J. van Meter, Phys. Rev. Lett. **96**, 111102 (2006), gr-qc/0511103.
- [8] C. O. Lousto and Y. Zlochower, Phys. Rev. Lett. **106**, 041101 (2011), arXiv:1009.0292 [gr-qc].
- [9] C. O. Lousto, H. Nakano, Y. Zlochower, and M. Campanelli, Phys. Rev. **D82**, 104057 (2010), arXiv:1008.4360 [gr-qc].

- [10] N. E. Rifat, S. E. Field, G. Khanna, and V. Varma, Phys. Rev. D **101**, 081502 (2020), arXiv:1910.10473 [gr-qc].
- [11] M. van de Meent and H. P. Pfeiffer, (2020), arXiv:2006.12036 [gr-qc].
- [12] C. O. Lousto and J. Healy, Phys. Rev. **D99**, 064023 (2019), arXiv:1805.08127 [gr-qc].
- [13] H. Nakano, J. Healy, C. O. Lousto, and Y. Zlochower, Phys. Rev. **D91**, 104022 (2015), arXiv:1503.00718 [gr-qc].
- [14] O. Dreyer, B. Krishnan, D. Shoemaker, and E. Schnetter, Phys. Rev. **D67**, 024018 (2003), gr-qc/0206008.
- [15] J. Healy, C. O. Lousto, and N. Rosato, (2020), arXiv:2003.02286 [gr-qc].
- [16] L. E. Kidder, C. M. Will, and A. G. Wiseman, Phys. Rev. **D47**, 3281 (1993).
- [17] C. O. Lousto and Y. Zlochower, Phys. Rev. **D77**, 024034 (2008), arXiv:0711.1165 [gr-qc].
- [18] J. Healy, C. O. Lousto, and Y. Zlochower, Phys. Rev. **D96**, 024031 (2017), arXiv:1705.07034 [gr-qc].
- [19] C. J. Woodford, M. Boyle, and H. P. Pfeiffer, Phys. Rev. **D100**, 124010 (2019), arXiv:1904.04842 [gr-qc].
- [20] J. Healy and C. O. Lousto, (2020), arXiv:2007.07910 [gr-qc].
- [21] J. Healy, C. O. Lousto, and Y. Zlochower, Phys. Rev. **D90**, 104004 (2014), arXiv:1406.7295 [gr-qc].
- [22] A. Ori and K. S. Thorne, Phys. Rev. **D62**, 124022 (2000), arXiv:gr-qc/0003032.
- [23] J. Healy and C. O. Lousto, Phys. Rev. **D95**, 024037 (2017), arXiv:1610.09713 [gr-qc].
- [24] A. Bohé *et al.*, Phys. Rev. **D95**, 044028 (2017), arXiv:1611.03703 [gr-qc].
- [25] I. Ruchlin, J. Healy, C. O. Lousto, and Y. Zlochower, Phys. Rev. **D95**, 024033 (2017), arXiv:1410.8607 [gr-qc].
- [26] Aristotle, *Physics*, Vol. VI:9 (350BCE) p. 239b10.
- [27] J. L. Borges, *Collected Fictions* (Penguin Classics Deluxe Edition, London, 1999).